Enhancement of Near Field GB-SAR Image Quality Using Beamwidth Filter

Enes Yigit[1], Umut Özkaya[2], Şaban Öztürk[3]

[1] Karamanoğlu Mehmetbey Üniversitesi, Mühendislik Fakültesi, Elektrik Elektronik Mühendisliği Bölümü; Karaman, Türkiye (ORCID: 0000-0002-0960-5335)
[2] Department of Electrical Electronics Engineering, Engineering Faculty, Konya Technical University, Konya, Turkey (ORCID: 0000-0002-9244-0024)
[3] Amasya University, Technology Faculty, Electrical and Electronics Engineering Department, Amasya, Turkey (ORCID: 0000-0003-2371-8173)

Abstract

In this study, the antenna beamwidth filter (ABF) was used to eliminate the image noise and clutter originating from the back-projection algorithm (BPA) used in near field ground-based synthetic aperture radar (GB-SAR) imaging. Since BPA interpolates the range profile obtained in each synthetic aperture onto the region to be imaged, it spreads the scattering collected in the beamwidth of the antenna to the whole region and as a result, noise occurs in the focused image. Thanks to the simple but effective technique presented in the study, each range profile was spread only to the area where the antenna beam corresponds to, and a noise-free and very clean radar images have been obtained. The effectiveness of the ABF was first verified with the simulation data and then two different real experiments were carried out. Both simulation and real measurements were carried out with step frequency continuous wave radar form. In the first experiment, because the synthetic aperture was relatively short and there was no dominant scatterer other than a metal reflector in the scene, very high image distortions did not occur between the traditional BPA and the filtered BPA results. Dispite these results, there were visually noticeable distortions that occurred in the focusing of the target and noisy signs appeared in the imaged scene. In the second experiment, quite notable differences were observed between filtered and traditional BPA results, as the scan was performed over a relatively long distance and there were too many scatterers in the target area. In the image reconsctructed using filtered BPA, while all targets were focused with high resolution and high contrast, in the image obtained by traditional BPA, it was observed that some small targets disappear under the noise signs. As a result of all these findings, it has been revealed that BPA with ABF has quite high performance and image quality.

Keywords: Back Projection Algorithm, Ground Based Synthetic Aperture Radar, Noise Removal, Antenna Beamwidth, Remote Sensing

Huzme Demet Filtresi kullanılarak Yakın Alan YT-SAR Görüntü Kalitesinin İyileştirilmesi

Öz

Bu çalışmada, yakın-alan yer tabanlı sentetik açıklıklı radar (GB-SAR) görüntülemede kullanılan geri projeksiyon algoritmasından (BPA) kaynaklanan görüntü gürültüsünü ve karmaşayı ortadan kaldırmak için anten ışın genişliği filtresi kullanılmıştır. BPA her bir sentetik açıklıkta elde edilen menzil profilini, görüntülenecek bölge üzerine interpole ettiği için, antenin huzme genişliği içinde toplanan saçılımları tüm bölgeye yaymakta ve bunun sonucu odaklanmış görüntüde gürültü oluşmaktadır. Çalışmada sunulan basit ama etkili teknik sayesinde, her bir menzil profili sadece anten ışın demetinin karşılık geldiği bölgeye yayılarak gürültüsüz ve oldukça temiz bir radar görüntüsü elde edilmiştir. Anten ışın demet filtresinin etkinliği öncelikle benzetim sonuçları ile doğrulanmış ardından 2 farklı gerçek deney gerçekleştirilmiştir. Hem benzetim deneyleri hemde gerçek ölçümler, adım frekans sürekli dalga radar formu ile gerçekleştirilmiştir. Birinci deneyde sentetik açıklık göreceli olarak kısa olduğu ve hedeflenen bölgede metal yansıtıcı dışında herhangi bir baskın yansıtıcı bulunmadığı için, geleneksel BPA sonucu ile filtreli BPA sonuçları arasında çok yüksek görüntü bozulmaları meydana gelmemiştir. Buna rağmen hedefin odaklanmasında görsel olarak farkedilir bozulmalar oluşmuş ve görüntülenen sahnede gürültü işaretleri ortaya çıkmıştır. İkinci deneyde nisbeten uzun bir mesafede tarama yapıldığı ve taranan bölgede çok fazla saçıcı bulunması nedeniyle, filtreli ve filtresiz BPA sonuçları arasında oldukça dikkate değer farklar gözlemlenmiştir. Filtreli BPA sonucu elde edilen görüntüde tüm hedeflerin yüksek çözünürlüklü ve yüksek kontrastla odaklanırken, filtresiz BPA sonucu elde edilen görüntüde

bazı küçük hedeflerin gürültüde kaybolduğu gözlemlenmiştir. Tüm bu çalışmalar sonucu, ışın demet filtreli BPA'nın oldukça yüksek performansa ve görüntü kalitesine sahip olduğu ortaya konulmuştur.

Anahtar Kelimeler: Geriye İzdüşüm Algoritması, Yer tabanlı Sentetik Açıklıklı Radar, Gürütlü Giderme, Anten huzme Demeti, Uzaktan algılama

1. Introduction

Synthetic Aperture Radar (SAR) is a signal processing technique generally used to obtain high-resolution electromagnetic scattering images of ground or underground targets with air or space-based systems. Such SAR systems are generally complex and expensive due to the costly platform requirements. On the other hand, in some remote sensing applications, rapid exploration of a small area of the earth with compact, low-cost high-resolution imaging sensors are desired. Examination of man-made and natural objects such as bridges, tunnels, cave entrance, water canal, underground mines, foreign object debris on airport runways, highway, vegetation cover, river, etc. are examples of these applications [1-4]. In recent years, Ground-Based SAR (GB-SAR) imaging techniques have been emphasized for the earth observation applications, and many studies have been carried out with various radar assemblies and equipment [3, 4]. In conventional SAR applications, since the distance between the antenna and target is far enough, EM wave propagation equations are solved by using far-field approximations. In the far field region, since the EM wave has a planar structure, the solutions of the backscatter equations are easy. However, in the near field, plane wave approaches are invalid and spherical wave propagation equations should be used. Since most of the GB-SAR applications are implemented in the near field region, SAR image reconstruction algorithms should be adapted to the near field region. For this reason, many useful approaches used in far field solutions cannot be used in near field region solutions. However, some SAR image reconstruction algorithms that exist in the literature can work flawlessly in near field applications due to their nature. Matched Filter Algorithm (MFA) [5], Back Projection Algorithm (BPA) [6], and Omega-K Algorithm (wkA) [7] are among the techniques that are frequently used in GB-SAR applications. Although these techniques have advantages and disadvantages compared to each other, it has been demonstrated that BPA is superior to others for near field applications [1].

BPA is a technique that creates images by superimposing 2-dimensional projections of each range profile collected along to the synthetic aperture to the coordinate axis to be displayed. As long as the cross-range length of the region to be imaged does not exceed the antenna beamwidth, highly successful focusing is achieved. However, as the scanning distance exceeds the beamwidth, the scattering signals in the range direction cause noise in the focused image. As a result, some targets cannot be detected in the focused image. In this study, using the ABF [8], this deficiency in BPA has been corrected. While the details of BPA and beam filtering method are given in the next section, the results of real GB-SAR applications are presented in the third section. In the last section, the study is summarized and the performance of the presented technique is evaluated.

2. Material and Method

2.1. Back Projection Algorithm

For the 2D scanning geometry as in Figure 1, while the instantaneous position of the radar antenna is defined by (X_n, Y_n), the $\overrightarrow{u_n}$ unit vector is a defined from the image center towards the instantaneous position of the antenna. The angle between the unit vector at any position of the antenna and the y axis in the range direction is defined by θ_n.
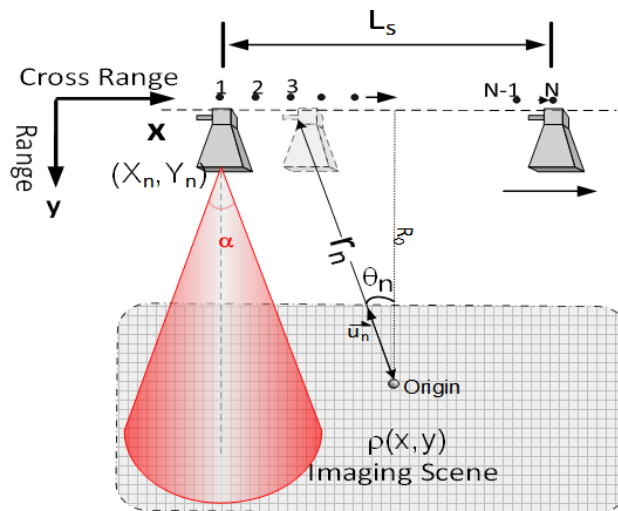

Figure 1. 2D SAR data acquisition geometry

According to these definitions, the 2D backscattering signal reflected from the targeted area along the entire aperture and collected by the antenna is expressed as follows

$$S(t_n, f_m) = E_{\theta_n}(k_r) = \int_{-\infty}^{+\infty} \int_{-\infty}^{+\infty} \rho(x,y).e^{-jk_r r_n} dx dy \qquad (1)$$

where k_r is the radial spatial frequency, denoting the bidirectional propagation and formulated as $k_r = \frac{4\pi f}{c}$ and c is the speed of light. $\rho(x, y)$ is the reflectivity function of the targeted region. r_n defines the distance from the current position of the antenna to any point (x, y). The distance of any point in the area to be imaged from the SAR antenna is analytically expressed as follows;

$$r_n = \sqrt{(X_n - x)^2 + (Y_n - y)^2} \tag{2}$$

where X_n and Y_n are the positions of the antenna relative to the image center, x and y are the coordinate information of each pixel of the region to be imaged. The range profile of the region illuminated electromagnetically is obtained taking the inverse Fourier Transform (IFT) of Equation 1 as follows,

$$e_{\theta_n}(r) \equiv IFT\{E_{\theta_n}(k_r)\} = \int_{-\infty}^{+\infty} \int_{-\infty}^{+\infty} \rho(x, y).\delta(r_n - r) dx dy \tag{3}$$

The expression of representing the scene in the 1D range profile for any observation point θ_n in Equation 3 is known as the Radon Transformation. At this point BPA starts with the IFT of the reflectivity function $\rho(x, y)$ given in Cartesian coordinates.

$$\rho(x, y) = \int_{-\infty}^{+\infty} \int_{-\infty}^{+\infty} G(k_x, k_y). e^{j(k_x x + k_y y)} dk_x dk_y \tag{4}$$

where the Fourier Transform (FT) of $\rho(x, y)$ is expressed by $G(k_x, k_y)$. Since the spatial frequency data is collected in polar coordinates, Equation 4 can be rewritten in terms of polar coordinates (k_r, θ_n) as follows.

$$\rho(x, y) = \int_{-\pi}^{+\pi} \int_0^{+\infty} G(k_r, \theta_n). \exp(jk_r r_n) k_r dk_r d\theta_n \tag{5}$$

At this point, the Projection-slice theorem [9] is used to associate the FT of the targets with the measurement data $E_\theta(k_r)$. The theorem simply states that the 1D FT of the projection at any angle represents the cross section of the 3D FT of the projection at the same angle, $E\_\theta (k\_r) \equiv G (k\_r, \theta)$. Using this principle, the Equation 5 can be rewritten as follows;

$$\rho(x, y) = \int_{-\pi}^{+\pi} \left[\int_0^{+\infty} E_{\theta_n}(k_r) \exp(jk_r r_n) k_r dk_r \right] d\theta_n \tag{6}$$

The inner integral in Equation 6 can be regarded as the 1D IFT of the $Q_{\theta_n}(k_r) = E_{\theta_n}(k_r) k_r$ function evaluated at r_n. If $q_{\theta_n}(r)$ is defined as the IFT of this function, Equation 6 can be expressed as

$$\rho(x, y) = \int_{-\pi}^{\pi} q_{\theta_n}(r_n) d\theta_n \tag{7}$$

Thus, the final form of the 2D BPA is obtained with Equation 7. The flow chart of traditional BPA is summarized in Figure 2a.
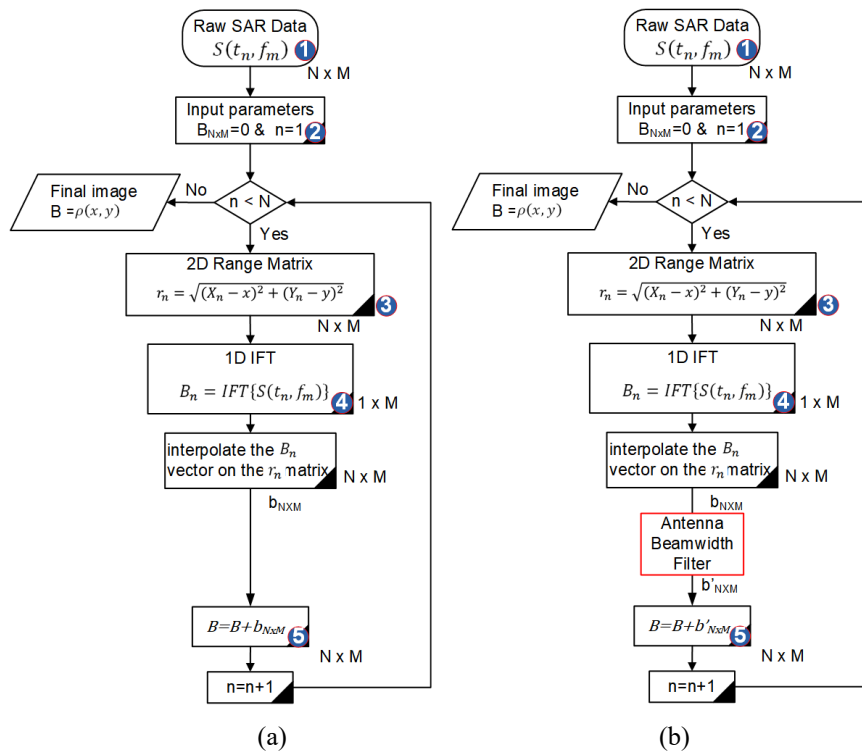
Figure 2. a) Flow chart of traditional BPA, b) Flow chart of BPA with beam filter

2.2 Antenna Beamwidth Filter for BPA

BPA, one of the SAR image focusing algorithms, performs the focusing procedure on range profiles corresponding to each synthetic aperture point. Each range profile is gathered harmoniously by spreading over a matrix grid framed with the dimensions of the region to be displayed.
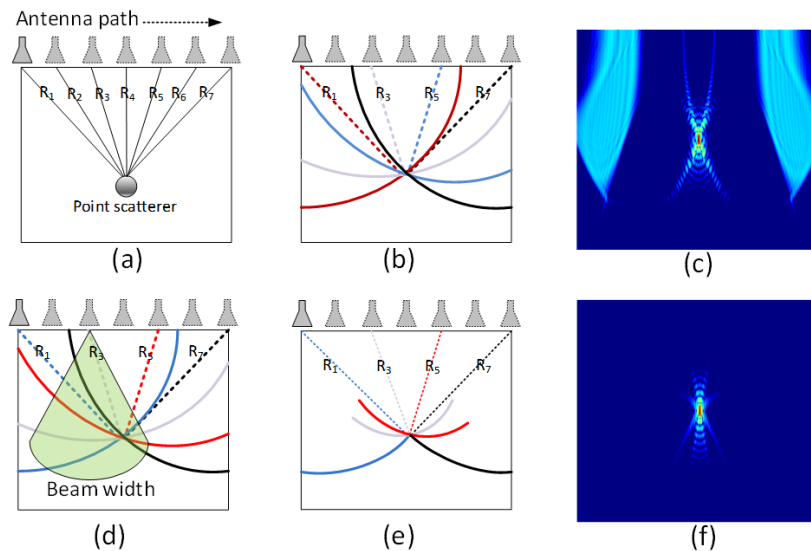

Figure 3. Graphical representation of the implementation of ABF; (a) Range distance at each synthetic aperture for point target, (b)Interpolation of range profile at each point to 2D grid, (c)Focused image after standard BPA (d) Use of antenna beamwidth filter, (e) New hyperbolic traces shortened at the end of the filter, (f) Focused image after filtered BPA

Figure 3a depicts the range lengths corresponding to each synthetic aperture during a standard SAR scan for a point target. Figure 3b shows how the BPA output works. As can be seen from Figure 3b, each range profile creates a hyperbolic arc when the range profile corresponding to each aperture is interpolated onto a new grid. When the arcs corresponding to each different aperture are gathered harmoniously on top of each other, the image focuses on the point where the target is located, as the amplitude at the target location suppresses other points. Figure 3c shows a reconstructed SAR image with a standard BPA. However, in the dynamic range of 30 dB, the effect of the side lobes shows themselves predominantly. However, when the antenna beam width is included in the algorithm with the proposed filtering, as seen in Figure 3d, the effects of the arcs outside of this beam are removed from the grid. Because in a real SAR application, while the antenna moves along to the fixed path, it collects target reflections across the beamwidth of the antenna.

Thus, after the filter is applied, as seen in Figure 3e, the dimensions of the arcs are restricted as the amount of the beamwidth. The reconstructed SAR image after filtering was acquired as a noiseless image as shown in Figure 3f.

Although the difference in simulation results for a point target is not much, in GB-SAR applications, backscatter effects from the whole area scanned by the antenna footprint are gathered in the range profile and distorts the focused image. For this reason, this filtering technique gives a very successful result in increasing the image quality in ground penetrating radar application using the SAR technique [10]. The ABF should be used after the 4th process step given in Figure 2a. According to this; for an antenna with α beamwidth, the angle γ between coordinates of the grid and the antenna is calculated as follows,

$$\gamma = \mathrm{acos}(\frac{y}{\sqrt{(X_n-x)^2+y^2}}) \tag{8}$$

where X_n indicates the location of the antenna, x and y are the range and cross range coordinates of the imaging area, respectively. After the γ matrix is obtained, ABF is performed by zeroing all values for $\gamma > \alpha$ for the B_{nm} matrix shown in Figure 2a. The flow chart of the ABF applied BPA is given in Figure 2b.

3. Results and Discussion

3.1. Simulation result

In order to test the effect of ABF on focusing quality, 14 ideal scatterers are positioned horizontally 3 m away from the scanning path as shown in Figure 4a. The coordinates of the targets are given in Figure 4a. The frequency of the stepped frequency continuous wave (SFCW) radar was changed between 4.5 GHz and 6 GHz in a total of 301 discrete points. Backscattering data were collected at 200 discrete synthetic aperture points along to the 4 m. The obtained raw GB-SAR data is given in Figure 4b, while the traditional BPA based reconstructed image is given in Figure 4c. In Figure 4c, it is seen that the point targets do not have a clear focus and the side-lobe signals cause very high noise in the image. On the other hand, in the image in Figure 4d reconstructed by filtered BPA, it is seen that the targets are focused with very high contrast.These results clearly demonstrate the effectiveness of the applied filter.
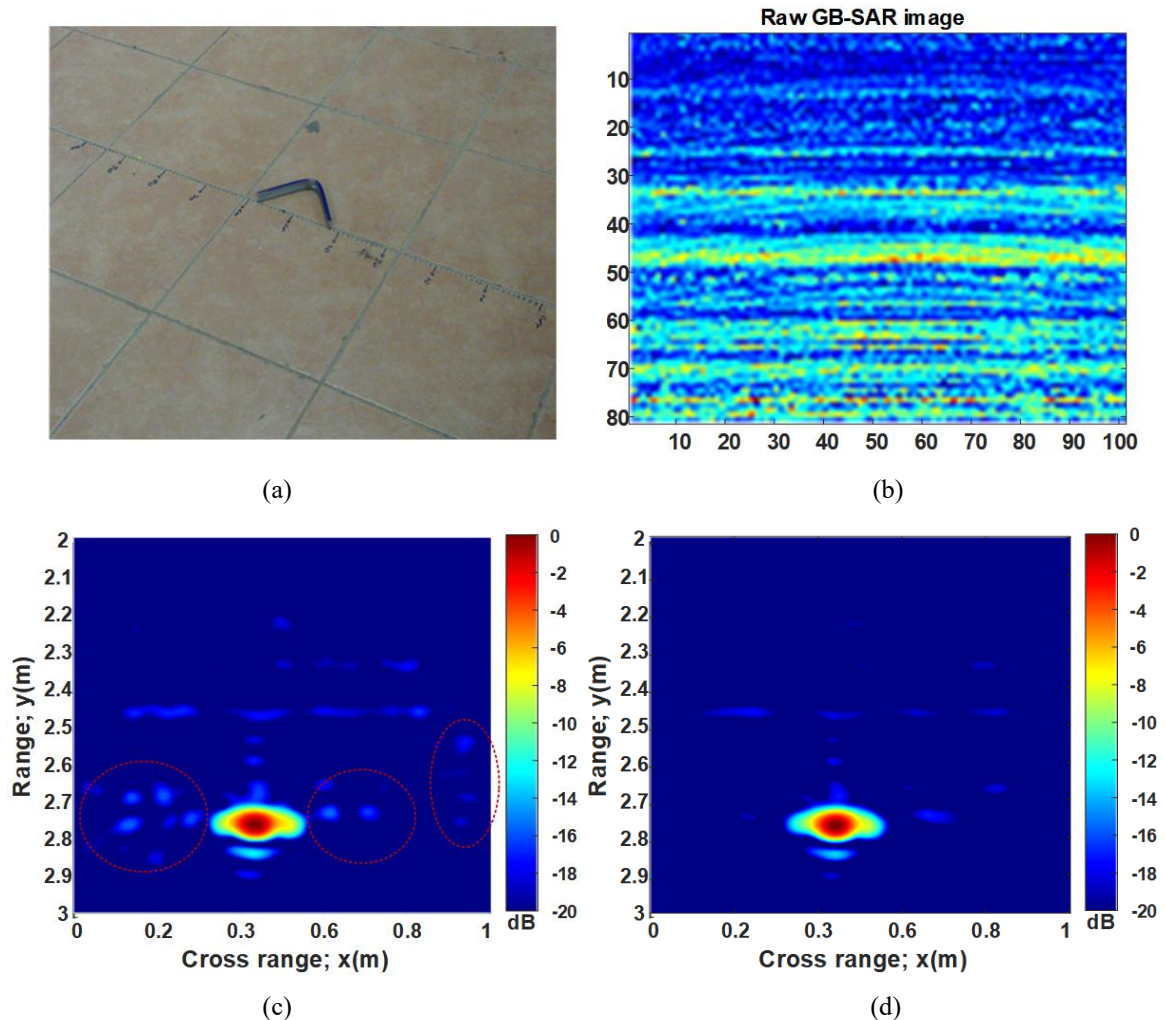

(a)

(b)

(c)

(d)
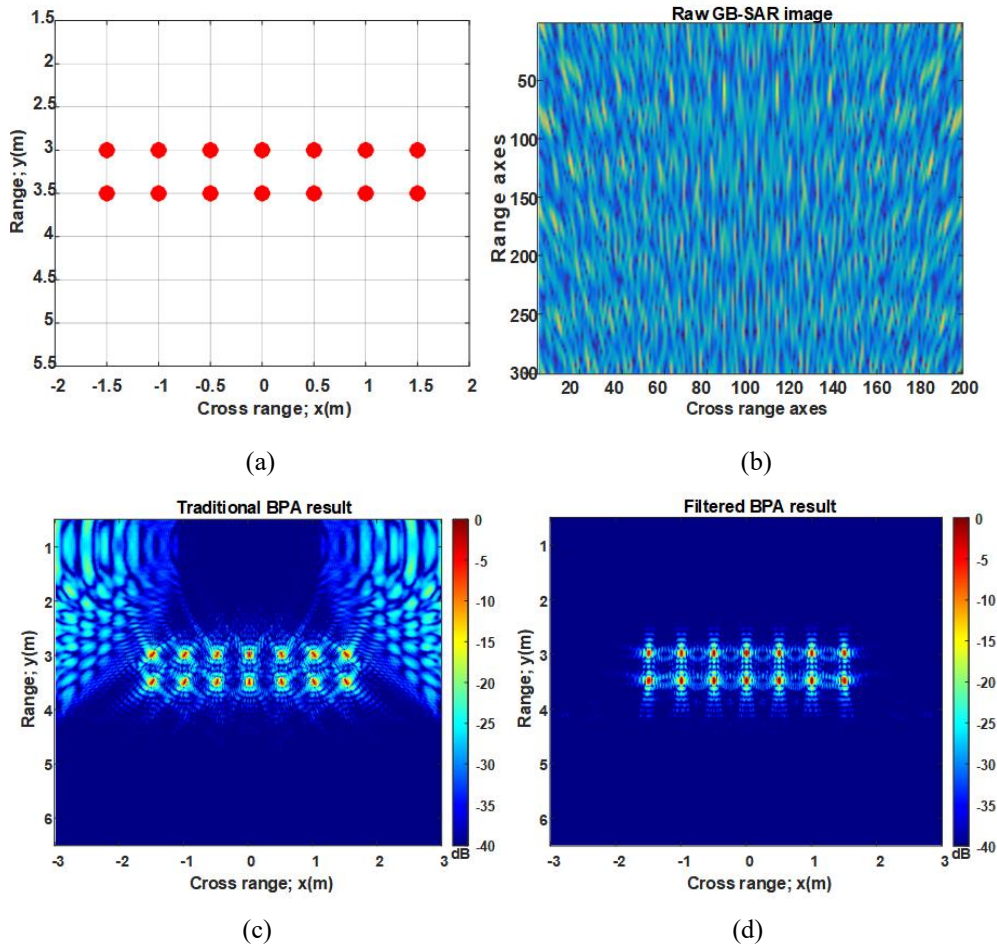
Figure 4. a) Hypothetical point targets, b) Spatial-frequency image of the GB-SAR system, c) Reconstructed image of the targets using traditional BPA, d) Reconstucted image of the targets using filtered BPA

3.2. Experimental results

Two different experiments were carried out in order to test the performance and efficiency of the ABF. SFCW data were gathered by Antritsu Handheld Vector Network Analyzer (VNA). Two C-band horn antennas having 24⁰ beamwidth and a wheeled platform that can hold the antennas were used to collect data. All measurements were carried out in the frequency range of 4.5 GHz to 6 GHz.

3.2.1. Expriment 1 (L shaped metal reflector)

For the performance test of the filtered BPA, an L-shaped metal object with a width of 15 cm as shown in Figure 5a was first located 2.8 m away from the antenna. The frequency of the VNA was changed between 4.5 - 6 GHz at 81 points. Backscattering data were gathered along a straight path of 1 m with 100 discrete spatial points. While the obtained raw spatial frequency GB-SAR image is given in Figure 5b, the reconstructed image with traditional BPA is given in Figure 5c.


(a)

(b)

(c)

(d)

Figure 5. a) L shaped metal target, b) Spatial frequency image of the GB-SAR data, c) Reconstructed image of the target using traditional BPA, d) Reconstucted image of the target using filtered BPA

The image obtained with the filtered BPA is shown in Figure 5d. When comparing Figures 5c and 5d, it is observed that in both figures the scattering mechanism of the target is focused at its true position, but the side-lobe reflections in the target region of the filtered BPA result are lower. However, the noise reflections within the red dotted circles given in Figure 5c are not present in Figure 5d. These results reveal how effective the applied filter is. In this experiment, since the background is uniform and is a single scatterer, relatively low noise signs occurred in the image obtained with conventional BPA. In order to compare the different environment performance of filtered BPA, a second experiment was conducted.

3.2.2. Experiment 2 (Highway imaging)

This measurement was carried out on a balcony 9 m above the ground, shown in Figure 6a. The backscattering data were gathered along a straight way of 10 m with 200 spatial points. For each spatial point, the frequency of the VNA was changed from 4.5 to 6 GHz with 5 MHz frequency steps to have a total of 301 discrete frequency points. While the reconstructed raw GB-SAR image using traditional BPA is given in Figure 6b, the filtered BPA result is shown in Figure 6c. When the Figure 6b is examined, it is seen that scattering points such as the pavements, vehicle reflectors, and trash bin are focused in their real places, but there is quite a lot of noise in the image. However, when comparing Figures 6b and 6c, it is seen that the reflectors on the road are hardly visible in Figure 6b, but

are very clear in Figure 6c. Also, the noise difference between both images is visually observed and this result reveals the superiority of the applied technique. When Figure 6b is examined, it is seen that there is more noise and clutter in the areas close to the antenna path, and these distortions decrease away from the antenna path. Therefore, the necessity of using an ABF in near field imaging with BPA has been clearly demonstrated.
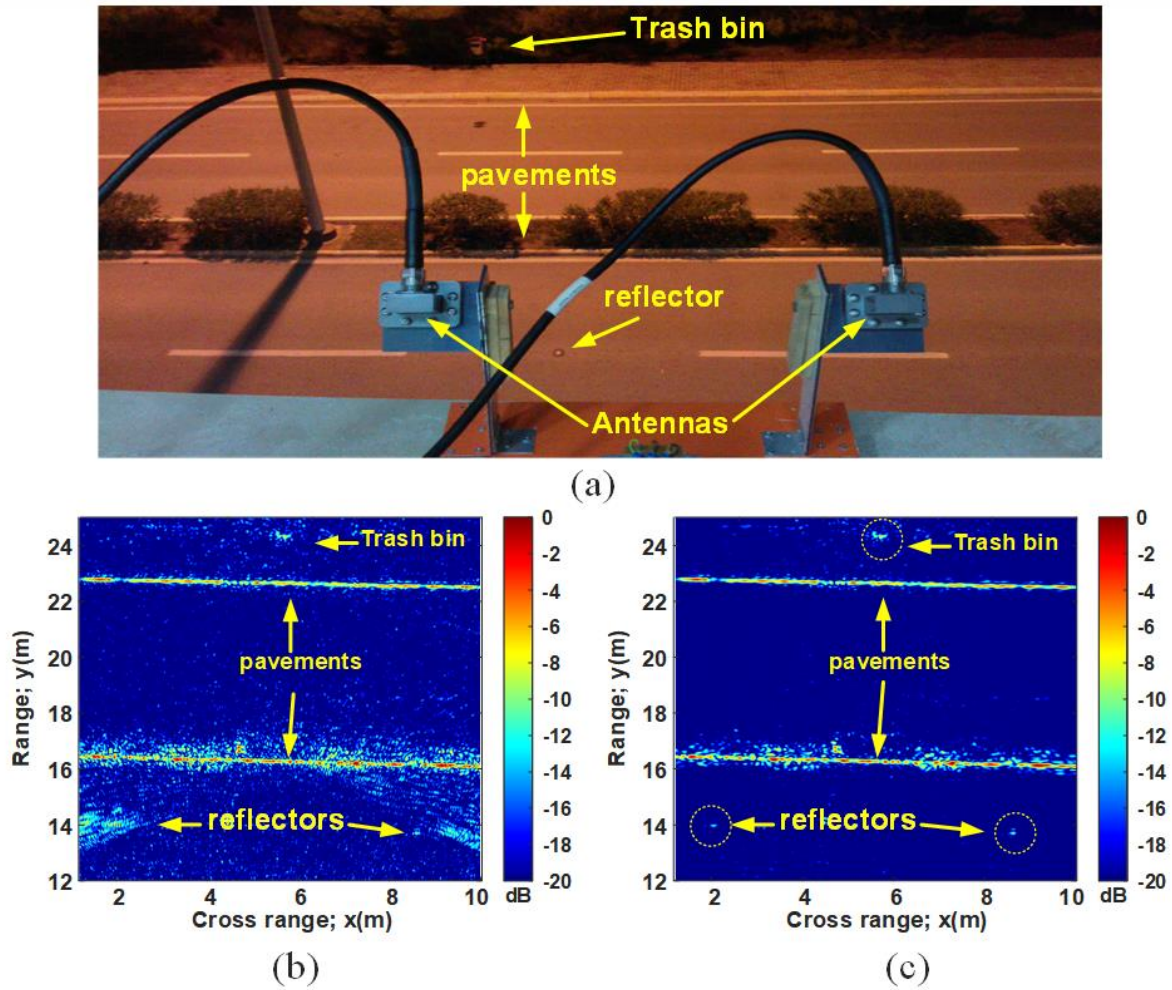
Figure 6. (a) Photograph of the scanned area during the highway experiment, (b) YT-SAR data focused on the unfiltered BPA result, (c) Focused YT-SAR data with filtered BPA

4. Conclusions and Recommendations

In this study, the formulation of the back-projection algorithm (BPA), one of the most popular focussing algorithms used for near-field GB-SAR applications, is detailly given. Then, antenna beamwidth filter (ABF) which can be used effectively in BPA, is presented in detail. The efficiency of the ABF was first verified with the simulation results, then 2 different real experiments were carried out. Both simulation experiments and real measurements were carried out with step frequency continuous wave (SFCW) radar form. In simulation experiments, 14 hypothetical ideal point scatterers were positioned 3 m away from the antenna scanning path and the frequency of the SFCW radar was changed between 4.5 and 6 GHz in a total of 301 points. Anritsu handheld vector network analyzer and 2 horn antennas in a quasi-bistatic configuration were used in real measurements. Real GB-SAR experiments were carried out between 4.5 GHz and 6 GHz. In the first experiment, a single metal target was positioned at a distance of 2.7 m from the antenna, while in the second experiment, GB-SAR data of a highway were collected across a synthetic aperture of 10 m. In both simulation and real application results, it was seen that filtered BPA completely cleans the unwanted sidelobes in the image and focuses the targets with very high contrast. With this study, the necessity of using an antenna beam filter in the use of BPA in near field SAR applications has been clearly demonstrated. In the light of these results, it is foreseen that filtered BPA will provide very clean focus performance in any near field application based on the SAR principle.

4. Acknowledge

References

[1] Yigit E, Demirci S, Ozdemir C, Tekbas M. Short-range ground-based synthetic aperture radar imaging: performance comparison between frequency-wavenumber migration and back-projection algorithms. J. Appl. Remote Sensing. 2013;7(1): 073483 – 073483

[2] M. Pieraccini, G. Luzi, D. Mecatti, L. Noferini and C. Atzeni, " Ground-based SAR for short and long term monitoring of unstable slopes " Proceedings of the 3rd European Radar Conference, 92- 95 (2006).

[3] Yigit E, Demirci S, Unal A, Ozdemir C, Vertiy A. Millimeter-wave ground-based synthetic aperture radar imaging for foreign object debris detection: experimental studies at short ranges. J. Infrared Millimeter Terahertz Waves. 2012;33(12):1227 – 1238.

[4] S.P Beasly, G. Binns, R. Hodges, R.J Badley, Tarsier., " A Millimetre Wave Radar for Airport Runway Debris Detection " , in Proc. of EURAD ' 04, Amsterdam (2004).

[5] Yigit E, Unal A, Demrici S, Vertiy A, Ozdemir C. An adapted mathced filter algorithm for millimeter wave ground based squint mode SAR applications, 2011 International Conference on Infrared, Millimeter, and Terahertz Waves, DOI: 10.1109/irmmw-THz.2011.6105117

[6] Demirci S, Çetinkaya H, Yigit E,Ozdemir C, Vertiy A. A Study on Mıllımeter-Wave Imagıng Of Concealed Objects: Applıcatıon Usıng Back-Projectıon Algorıthm, Progress In Electromagnetics Research, Vol. 128, 457–477, 2012

[7] Yigit E, Demrici S, Ozdemir C, Kavak A. A Synthetıc Aperture Radar-Based Focusıng Algorıthm For B-Scan Ground Penetratıng Radar Imagery, Mıcrowave And Optıcal Technology Letters / Vol. 49, No. 10, 2007

[8] Yigit E. Construction of synthetic aperture radar system for ground platforms and obtaining real terrestrial radar images, Phd. Thesis, Mersin University, Institute of Science. 2013.

[9] Mersereau R, Oppenheim "A. Digital reconstruction of multidimensional signals from their projections". P IEEE, 62(10): 1319–38, (1974).

[10] Demirci S. Yigit E. Eskidemir I.H, Ozdemir C. Ground penetrating radar imaging of water leaks from buried pipes based on back-projection method, NDT&E International 47 (2012) 35–42